

Geophysical Research Letters[®]



RESEARCH LETTER

10.1029/2024GL108864

Implications of Variability and Trends in Coastal Extreme Water Levels

William V. Sweet¹ , Ayesha S. Genz² , Melisa Menendez³, John J. Marra², and Jayantha Obeysekera⁴

¹National Oceanic and Atmospheric Administration, National Ocean Service, Silver Spring, MD, USA, ²National Oceanic and Atmospheric Administration, National Centers for Environmental Information, Honolulu, HI, USA, ³IHCantabria—Instituto de Hidráulica Ambiental de la Universidad de Cantabria, Santander, Spain, ⁴Sea Level Solutions Center, Florida International University, Miami, FL, USA

Key Points:

- Probability distributions of coastal extreme water levels shift higher and lower with tide cycles, climatic patterns and sea level rise (SLR)
- Annual shifts of >15 cm from variability along Pacific coasts exceed SLR over the last 30 years and projected over the next 30 years
- Annual-scale variability envelopes are envisioned to assist in decadal-scale SLR and flood frequency assessments

Correspondence to:

W. V. Sweet,
william.sweet@noaa.gov

Citation:

Sweet, W. V., Genz, A. S., Menendez, M., Marra, J. J., & Obeysekera, J. (2024). Implications of variability and trends in coastal extreme water levels. *Geophysical Research Letters*, 51, e2024GL108864. <https://doi.org/10.1029/2024GL108864>

Received 20 FEB 2024

Accepted 18 JUN 2024

Author Contributions:

Conceptualization: Ayesha S. Genz, Melisa Menendez, John J. Marra, Jayantha Obeysekera
Formal analysis: Ayesha S. Genz, Melisa Menendez, Jayantha Obeysekera
Funding acquisition: John J. Marra
Investigation: Melisa Menendez
Methodology: Ayesha S. Genz, Melisa Menendez, Jayantha Obeysekera
Software: John J. Marra
Writing – review & editing: John J. Marra, Jayantha Obeysekera

Abstract Probabilities of coastal extreme water levels (EWLs) are increasing as sea levels rise. Using a time-dependent statistical model on tide gauge data along U.S. and Pacific Basin coastlines, we show that EWL probability distributions also shift on an annual basis from climate forcing and long-period tidal cycles. In some regions, combined variability (>15 cm) can be as large or larger than the amount of sea level rise (SLR) experienced over the past 30 years and projected over the next 30 years. Considering SLR and variability by 2050 at a location like La Jolla, California suggests a moderate-level (damaging) flood today with a 50-year return level (2% annual chance) would occur about 3–4 times a year during an El Niño nearing the peak of the nodal tide cycle. If interannual variability is overlooked, SLR related impacts could be more severe than anticipated based solely upon decadal-scale projections.

Plain Language Summary Coastal communities are flooding more often due to sea level rise (SLR), but some years are worse than others. We use a statistical model to show how the probabilities of coastal high waters, often referred to as extreme water levels—a combination of above average tides and storm surge—have shifted higher or lower every year with SLR and from changes in the tides and climatic (persistent weather and ocean) patterns. There are many U.S. and Pacific coastal regions where year-to-year variability is 15 cm or more, which is as large as the last 30 years of SLR and this pattern is projected to continue over the next 30 years. Considering additional SLR over the next 30 years could help compensate for year-to-year variability.

1. Introduction

As sea levels rise, so are concerns about the growing impacts of coastal flooding and erosion (Collini et al., 2022; Fox-Kemper et al., 2021; Hall et al., 2016; Marra et al., 2023; May et al., 2023). For good reason, as annual frequencies of high tide (aka nuisance, king-tide, or sunny-day) flooding, which are mostly minor/disruptive in nature are already accelerating along many U.S. and global coastlines (Fox-Kemper et al., 2021; Sweet & Park, 2014; P. R. Thompson et al., 2023). When estimating future changes in flood frequencies or exposure, common practice is to combine sea level rise (SLR) projections with observed or modeled probability distributions of extreme water levels (EWLs) (Buchanan et al., 2017; Church et al., 2013; Ghanbari et al., 2019; Hunter, 2012; Karegar et al., 2017; Kopp et al., 2014; Moftakhari et al., 2015; Muis et al., 2016; Oppenheimer et al., 2019; Taherkhani et al., 2020; Tebaldi et al., 2012; Vitousek et al., 2017; Vousdoukas et al., 2018; Wahl & Chambers, 2016; Wahl et al., 2017) as shown in Figure 1a. But other factors are also at play, which can further intensify the typical seasonality of high tide flooding (Dusek et al., 2022; Sweet et al., 2018; P. R. Thompson et al., 2021). In some years, climate forcing such as associated with the El Niño Southern Oscillation (ENSO) and changing astronomical tide heights affect sea levels, storm tracks, and flood frequency (Figure 1b; Barnard et al., 2015; Li et al., 2022; Haigh et al., 2011; Menéndez & Woodworth, 2010; Méndez et al., 2007; Rashid & Wahl, 2020; Rashid et al., 2019; Sweet & Park, 2014; Sweet & Zervas, 2011; P. R. Thompson et al., 2013, 2021). If interannual variability is overlooked, EWL frequencies over the next several decades could be underestimated if not accounted for in SLR assessments.

Here, we use a probabilistic framework to diagnose past trends and interannual variability affecting EWLs along U.S. coastlines and those of the Pacific Basin surrounding U.S. Island territories and interests. An outlook for the next 30 years (2050 relative to 2020) is given considering the U.S. Intermediate Low SLR scenario (Sweet et al., 2022), which represents a 0.5-m global SLR by 2100 and varies locally per the AR6 IPCC framework (Fox-

© 2024. The Author(s).

This is an open access article under the terms of the [Creative Commons Attribution License](https://creativecommons.org/licenses/by/4.0/), which permits use, distribution and reproduction in any medium, provided the original work is properly cited.

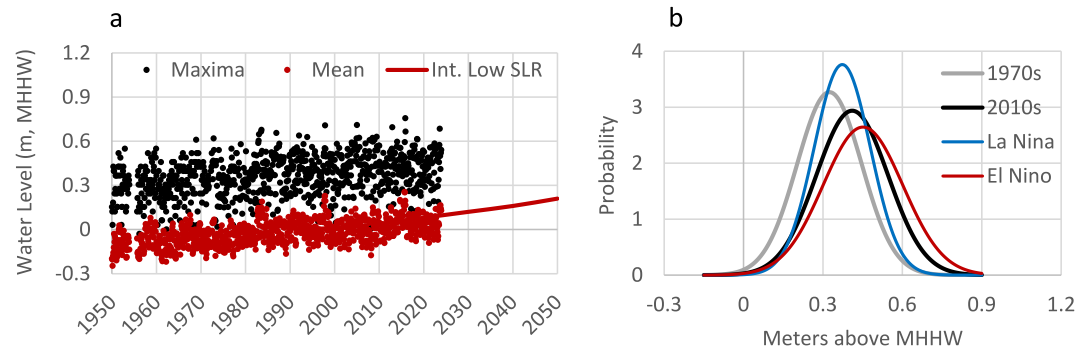


Figure 1. (a) Monthly maxima and mean water levels in La Jolla, California showing the U.S. Intermediate Low sea level rise (SLR) scenario of Sweet et al. (2022). In (b) are probability distributions of monthly water level maxima fit (normally distributed for illustrative purposes) to monthly maxima data in the 1970s and 2010s and for specific years of La Nina (1984, 1999, 2011) and El Nino (1982, 1997, 2015) highlighting how SLR and climatic patterns have temporal dependencies modeled in this study. The nodal cycle is not highlighted here in (b). The extreme water level distribution at La Jolla shifts 4.2 cm per unit measure of El Nino Southern Oscillation assessed in this study.

Kemper et al., 2021). The current SLR trajectories extrapolated to 2050 along most regional U.S. coastline are close to this scenario except along the Southeast Atlantic and Gulf coasts where they are about 5–10 cm higher than the Intermediate Low levels (Hamlington et al., 2022; Sweet et al., 2022 for details) possibly due to decadal-scale variability (Dangendorf et al., 2023). In general, the Intermediate Low SLR is considered *likely* to be exceeded by the end of century based upon global temperature/emission commitments to date (Riahi et al., 2022). The 2050 outlook also considers combined variability from the moon's nodal tide cycle as recently examined by P. R. Thompson et al. (2021) and builds on this work by (a) attributing variability to global climatic patterns and (b) quantifying how the full envelop of EWL probabilities have responded through time. Since this study focuses on tide gauge data, it does not explicitly include wave effects that are often times the main driver of over wash, erosion and flooding along many Pacific coastlines (Barnard et al., 2019; May et al., 2023; Shope et al., 2022; Storlazzi et al., 2018; Vitousek et al., 2017). The outcomes are presented in terms of changes to a rare event like the 50-year return level (Menéndez & Woodworth, 2010; Obeysekera & Salas, 2020; Salas et al., 2018; Vitousek et al., 2017) with contextualization using U.S. National Oceanic and Atmospheric Administration (NOAA) coastal flood height-severity thresholds.

2. Data and Methods

Time-dependent generalized extreme value (GEV) models (e.g., Menéndez & Woodworth, 2010; Menendez, Mendez, & Losada, 2009; Menendez, Mendez, Izaguirre, et al., 2009; Méndez et al., 2007) are applied to monthly maxima water levels from 1950 to 2020 for 168 tide gauges along U.S. and Pacific coastlines with data obtained from the University of Hawaii Sea Level Center (Caldwell et al., 2015) and NOAA (2023b). The EWLs in this study are considered stillwater levels (Moritz et al., 2015) as wave effects, though sensed by NOAA tide gauge (Kirk et al., 2022; Sweet et al., 2015) are not included in this study. Inclusion of wave effects (beyond the scope of this study), which have their own time-dependent qualities (e.g., Izaguirre et al., 2011; Méndez et al., 2006) and can be on the order of 25%–90% the overall total height of EWL along some coastlines (May et al., 2023) are important when assessing prone (e.g., U.S. West coast) coastlines (Lobeto et al., 2024; Serafin et al., 2017; Serafin & Ruggiero, 2014).

The GEV model has three parameters: a location parameter— μ (μ) that centers the distribution, a scale parameter— ψ (ψ) which represents the dispersion, and a shape parameter— ξ (ξ) that determines the shape of the upper tail and is expressed as:

$$G(x) = \left\{ \exp \left\{ - \left[1 + \xi \left(\frac{x - \mu(t)}{\psi} \right) \right]_+^{\frac{1}{\xi}} \right\}, \quad \xi \neq 0 \exp \left\{ - \exp \left[- \left(\frac{x - \mu(t)}{\psi} \right) \right] \right\}, \quad \xi = 0$$

with a time-dependent (nonstationary) location parameter that models how the distribution shifts with intra-annual seasonal (S) cycles, an 18.6-year tidal nodal ($T_N = 18.6$) cycle, influences of interannual climate patterns (cvte), and long-term trends (LT) and expressed as:

$$G(\mu(t), \psi, \xi) \Rightarrow \mu(t) = \mu_0 + \mu_S(t) + \mu_{LT}(t) + \mu_N(t) + \mu_{cvte}(t) \quad \text{with}$$

$$\mu_S(t) = \sum_{i=1}^3 [\beta_{2i-1} \cos(2i\pi t) + \beta_{2i} \sin(2i\pi t)]$$

$$\mu_{LT} = e^{(\beta_{LT}t)}$$

$$\mu_N(t) = \beta_{N1} \cos\left(\frac{2\pi t}{T_N}\right) + \beta_{N2} \sin\left(\frac{2\pi t}{T_N}\right)$$

$$\mu_{cvte}(t) = \beta_{cvte} \cdot Cvte(t)$$

Typically, the shape parameter is assumed to be fixed (Coles et al., 2001) as rare events like surges from land-falling tropical cyclones that often appear as “outliers” are sparse in tide gauge records. In our study, we assumed that both the shape and scale parameters (e.g., affecting seasonality or trends—if they exist—in “storminess”) are held constant for simplification. Also, the models do not include the 4.4-year cycle related to perigeon tide-cycle influences (Haigh et al., 2011) that can override the nodal cycle in some places (Menéndez & Woodworth, 2010). Time-dependent models were tested in a stepwise manner, starting with seasonal and trend in the location parameter, then including nodal, and lastly a climate variability index. A chi-squared deviance statistic ($\alpha = 0.05$) identifies the model for each tide gauge with the least number of parameters that best describes the data. Climate variability (cvte) representing large-scale persistent ocean and atmospheric patterns are quantified by monthly time series of the six major indices describing Pacific and Atlantic dynamics (NOAA, 2023a) including ENSO (a) via a bivariate ENSO time series (BEST; Smith & Sardeshmukh, 2000) and the Oceanic Niño Index (ONI; Barnston et al., 1997), (b) the Pacific Decadal Oscillation (PDO; Mantua et al., 1997), (c) the Pacific North American Index (PNA; Wallace & Gutzler, 1981), (d) the Tropical Northern Atlantic Index (TNA; Enfield et al., 1999), (e) the Arctic Oscillation (AO; D. W. J. Thompson & Wallace, 1998) and (f) the North Atlantic Oscillation (NAO; Hurrell, 1995). Only the most influential climate index is retained and presented. Lastly, the long-term trend is fit with an exponential to account for any acceleration if present.

The EWL probabilities highlighted here are shown as return level curves and range from the 100-year (1% annual chance level) to the 0.1-year (10 events per year) water levels using the approximation of $-1/\ln(G_x)$ instead of the traditional $1/(1 - G_x)$ method (Beran & Nozdryn-Plotnicki, 1977; Coles et al., 2001) to estimate sub-annual probabilities. Confidence intervals were computed using the delta method (Rice, 1994) and are similar to more-traditional stationary estimates (Menendez, Mendez, Izaguirre, et al., 2009; Méndez et al., 2007). However, since they are not the focus on this study, only the expected (median) values are shown. Also, the models quantify monthly probabilities, but we only show annualized probabilities to align with annual-to-decadal assessment purposes. Lastly, the rare event probabilities, for example, the 100-year return levels like those of NOAA (Zervas, 2013) are based upon a single gauge analysis and can differ from those quantified by FEMA (2016) that include simulated storms (Nadal-Caraballo et al., 2020).

3. Findings

These time-dependent statistical models disentangle stochastic (climate pattern) from deterministic (tide) from persistent (trend) forcing that affect (shift) the location parameter and the entire EWL distribution. In terms of climate variability (Figure 2b), ENSO has the largest footprint (Figure 2a), with many locations experiencing a 9–15+ cm effect along the Pacific North/South American and Island coastlines (12 ± 6 cm [median ± 1 standard deviation]). A 12-cm ENSO range equates to a location parameter shift of about 4.5 cm per unit ENSO index (e.g., the annual averaged ONI index has varied 2.7°C range over the study period). Other notable clusters include the AO effect along the Northeast U.S. coastline (3–6 cm), the PNA along the U.S. Alaskan coastline (9–15 cm) and the PDO along the Japanese coastline. The nodal tide component (<20-year period) is about 3–6 cm across the study region and locally higher where tide ranges are higher, for example, along the U.S. NW and Alaskan coastlines (Figure 2c). Lastly, the accumulated EWL trend amount over 1990–2020 (Figure 2d) is very close to

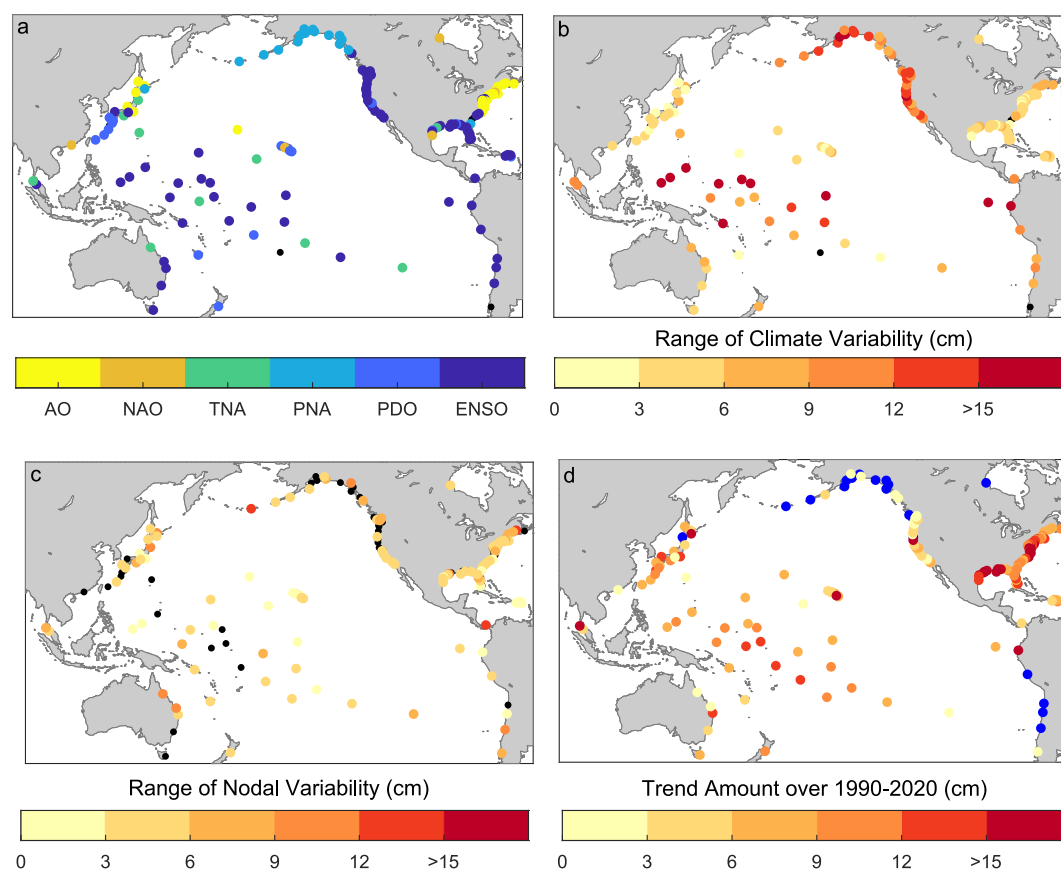


Figure 2. (a) The climate index with the highest influence on the location parameter and (b) its range (minimum to maximum) since 1950. In (c) is the range of the nodal range (black dots have no nodal influence) and in (d) is the amount of the extreme water level trend over the 1990–2020 period (blue dots indicate where the trend is negative).

mean sea level change over the same period (R -squared = 0.98 in a linear regression [EWL trends = 1.02 mean trends] across all tide gauge sites, not shown). Rise amounts reflect familiar SLR patterns, for example, high amounts (>15 cm) in the western equatorial Pacific and along the U.S. East and Gulf coasts largely from land subsidence issues. Decreases occur where rebound is occurring such as along the southern Alaskan coastline.

In terms of relative contributions, climate variability is more than twice that from the nodal cycle (nodal-to-climate variability ratio = 0.4 ± 0.7) assessed across all sites with ratios of 0.8 ± 0.7 , 0 ± 0.2 and 0.4 ± 0.6 along the U.S. Atlantic/Gulf, U.S. West and Pacific Island coasts, respectively. Also, the combined range of variability (climatic plus nodal) is about the same magnitude of the EWL trend over the last 30 years assessed across all sites (trend-to-variability ratio of 1.0 ± 1.6). There are some noted regional differences where the trends are relatively large like along the U.S. East and Gulf coasts (1.7 ± 1.9) or where variability is much higher like along the U.S. West coast (0.3 ± 0.3). Variability from both the nodal and climate components have combined to achieve about 90% of the full range at most locations and within a 15–20 year period.

Two tide gauges at La Jolla, CA and Boston, MA (Figure 3) exemplify the time-dependent changes of the location parameter and effects on the return levels. The 50-year return levels, higher in Boston (1.23 m above mean higher high water (MHHW)) than La Jolla (0.74 m above MHHW), are highlighted in Figures 3a and 3b. The time series of the 50-year levels reflect the combined effects of the three time-dependent components (Figures 3a and 3b) and show a higher climatic influence at La Jolla (11 cm) as compared to Boston (8 cm). However, the 30-year EWL trend amounts are higher (9 vs. 7.4 cm) in Boston than La Jolla, as is the nodal cycle (8 vs. 6 cm, respectively), which is nearly out of phase between locations. The stronger El Niño (e.g., 1982–1983, 1997–1998, 2009–2010, 2015–2016) are clearly evident in the La Jolla series. Though the 50-year level is illustrated, the same magnitude and time dependencies would apply to the entire probability distribution (affecting the 1-year, 10-year levels, etc.).

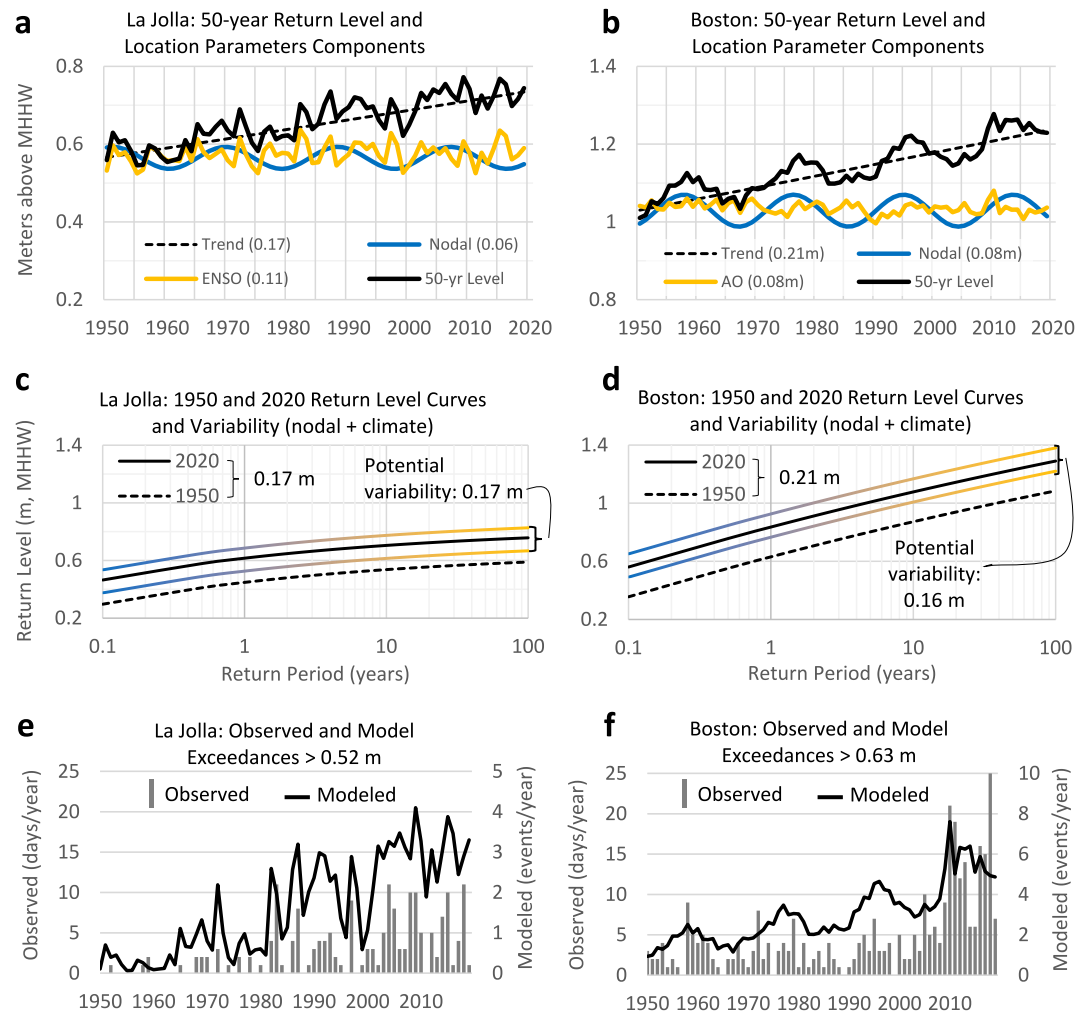


Figure 3. Highlighting at La Jolla and Boston the (a, b) time-dependent 50-year return level and contributions from climate and nodal variability and extreme water level trends. In (c) and (d) is the return level curve for 2020 (solid black line) and how the curves could conditionally vary by the combined nodal and climate variability (lines shown as a blend of yellow and blue representing both variability contributions as shown in (a) and (b)). Also shown are how the curves have changed since 1950 (black dash line) due to trends in the monthly maxima water levels (which closely track local sea level rise). In (e) and (f) are the sub-annual time-dependent model probabilities and high tide flooding observations, which reveal the ~19-year nodal cycle at Boston and El Nino Southern Oscillation (ENSO) effects at La Jolla.

The 2020 return level curves in Figures 3c and 3d show the influence (larger scale and shape parameter values—not shown) from stronger and more frequent winter storms and higher surges along Boston's wider and shallower continental shelf than La Jolla (Tebaldi et al., 2012). The 1-year level is higher in Boston than the 100-year level is in La Jolla. The EWL trend effects are also shown by highlighting the difference in the return level between 1950 and 2020. Also shown is an envelope about the 2020 return level curve representing the combined (nodal plus climate) variability that conditionally (if the nodal phase was different or a stronger ENSO or AO conditions occurred) could further shift the return level curves.

To provide a sensitivity assessment, the time-dependent probabilities are compared to annual high tide flood frequencies (Sweet et al., 2018) associated with minor/disruptive impacts measured by NOAA tide gauges (Figures 3e and 3f). The sub-annual probabilities from the model capture the main observational patterns, specifically ENSO effects at La Jolla and the nodal cycle at Boston with correlation values of 0.67 and 0.73 at La Jolla and Boston (not shown). The nature of the correlations (‘‘events’’) between the observations (days with an exceedance) versus the modeled results (‘‘events’’) is often characterized as accelerating (quadratic fit), implying that as the events become more routine, they last longer. The role of these time-dependent models is

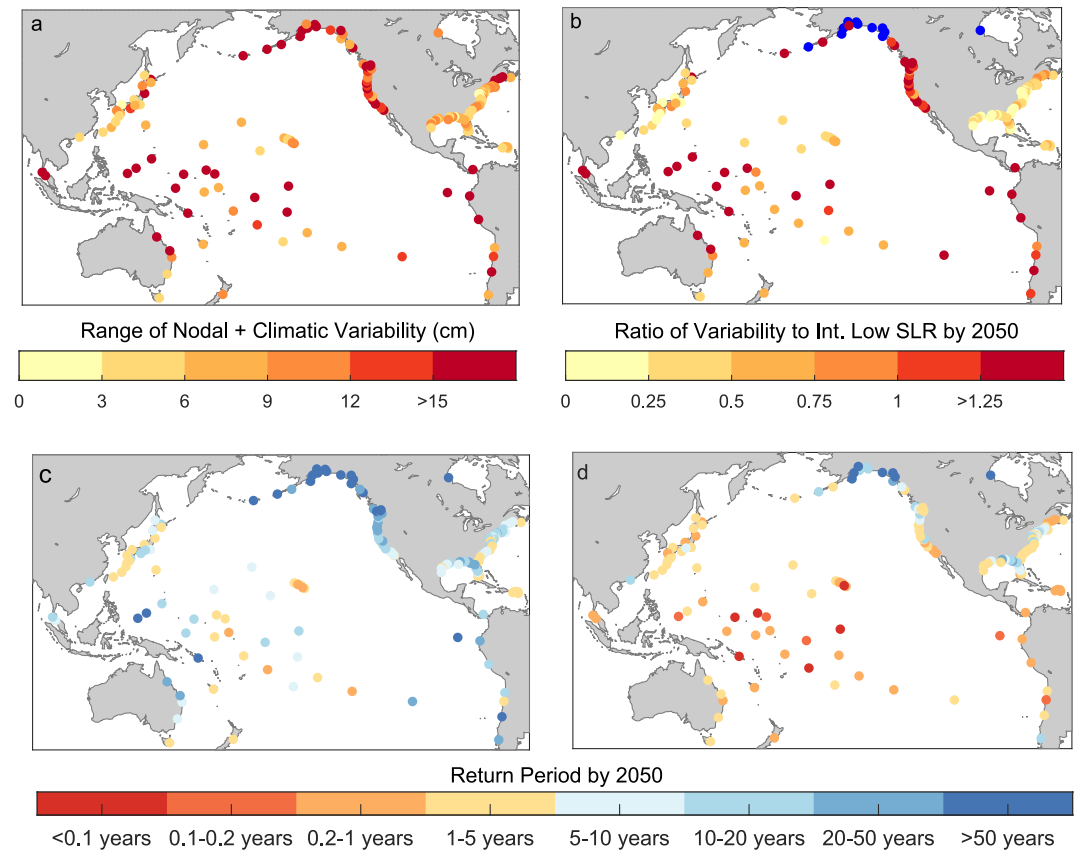


Figure 4. (a) The combined range in the location parameter of nodal and climate variability as in Figures 2b and 2c and (b) how this range relates to the sea level rise (SLR) by 2050 under the U.S. Intermediate Low SLR scenario (Sweet et al., 2022). Blue dots highlight locations where sea levels are projected to drop. The change in return periods in 2050 of the 50-year levels as estimated in 2020 are shown considering the (c) low-end range ($-1/2$ range) and (d) high-end range ($+1/2$ range) of the variability shown in (a) added to the 2050 SLR by 2050. Return periods less than 1 year, for example, 0.2 years, equals 5 events per year.

not necessarily for near-term prediction purposes of high tide flooding, which is a focus of NOAA's monthly-to-annual high tide flood prediction efforts (Dusek et al., 2022; Sweet et al., 2018). Though these models do provide some ability and skill for predicting a range of EWLs (Menendez, Mendez, & Losada, 2009), the focus is to assess climate variability and trend responses to develop a probabilistic envelope to help bound variability for decadal-scale assessments similar to what is done for sub-annual frequencies by P. R. Thompson et al. (2021).

Looking out to year 2050, the combined variability (Figure 4a; nodal + climatic) assessed across the entire study region is 9 ± 7 cm and less than half as much as SLR under the Intermediate Low SLR scenario (variability-to-SLR ratio of 0.4 ± 0.2). However, within the ENSO footprint along the Pacific North/South American and Island coastlines, the range of combined variability (16 ± 7 cm) is projected to be as large or larger as SLR under the Intermediate Low SLR scenario to 2050 relative/rebaselined to 2020 (ratio of 1.4 ± 0.7 ; Figure 4b). Rebaselining the SLR scenarios to 2020 from their 2000 origination is within about 1 cm based upon trend fits from 1970 to 2020 as assessed along U.S. coastlines (Sweet et al., 2022). Along the southern Alaskan coast, SLR under this scenario is projected to drop further by 2050, and thus variability will reach lower elevations than now. Along the U.S. East and Gulf coastlines, variability is about a third of the amount of SLR (ratio of 0.3 ± 0.2 ; Figure 4b). We note that not all EWL variability is necessarily diagnosed by our models. Using more customized indices (e.g., Rashid & Wahl, 2020) could help, like Gulf Stream transport and its 5–10 cm effect on EWL along South Florida coastlines (Sweet et al., 2016).

Considering the U.S. Intermediate SLR scenario instead (1 m global rise by 2100), the variability-to-SLR ratios assessed are nearly the same (e.g., 1 ± 0.5 in ENSO footprints along the Pacific North/South American and Island

coastlines) since there is only a 3.5 ± 1 cm SLR difference between the two scenarios in 2050 across the study region. In fact, there is not much divergence by 2050 across all of the U.S. SLR scenarios (Sweet et al., 2022) or the IPCC temperature-emission based projections (Fox-Kemper et al., 2021). An assumption about future changes for either SLR scenario is that EWL trends will continue to parallel those of mean sea level, similar to that observed over the last 30 years.

The time dependencies and their potential effects on flood frequencies are highlighted in the late 2040s, when coincidence of nodal peaks and potential climatic drivers could see many location's current 50-year return levels occurring multiple times a year. Assessed across all tide gauges, the range in return periods by 2050 considering the low-end (Figure 4c) to high-end (Figure 4d) range of variability centered about the Intermediate Low SLR projection is about 12 to 3 years, respectively. At regional scale, this equates to about a 10 to 6 years, a 24 to 4 years and a 5-to-0.3-year range in return periods along the U.S. East/Gulf, U.S. West and Pacific Island coasts, respectively. Considering specific locations like La Jolla and Boston, where the nodal cycle is set to peak about 2045 and 2050, respectively, this would translate to a 10-to-0.3-year and a 11-to-2-year range in return periods considering their current (2020) 50-year return levels. Thus, it is conceivable that by about 2050 if the nodal and climatic forcing align, La Jolla could experience 3–4 events in a year. For perspective, these 50-year return levels are close to the NOAA moderate coastal flood level in La Jolla and the major flood level at Boston, which equate to damaging (moderate) and destructive (major), respectively, in terms of impacts presenting a serious risk to property (moderate) and lives (major) (May et al., 2023; Sweet et al., 2018).

4. Concluding Remarks

The probability of EWL causing disruptive-to-destructive coastal flooding along many U.S. and Pacific Basin coastlines is growing due to decades' worth of SLR (Fox-Kemper et al., 2021; May et al., 2023). As observed along U.S. coastlines, annual frequencies of minor/disruptive high tide flooding are much more severe in some years than others (Sweet et al., 2018, 2021). EWL variability associated with global climate patterns and the nodal tide cycle are key factors and they have distinct regional patterns. Along the U.S. East and Gulf coasts, the two factors are about the same in terms of influence. However, along much of the Pacific North/South American and Island coastlines, ENSO and the PNA climatic variability is 2–3 times or more influential than the nodal tide cycle. Though the strongest historical climatic responses (peaks) have not always coincided with nodal peaks, they have come close (90% of full range at most locations) within about a 15–20 year period. Of particular importance is the combined (nodal + climate) variability along the Pacific North/South American and Island coastlines that is as large or larger (>15 cm) as the SLR projected over the next 30 years.

In terms of predicting future variability, climate forcing such as ENSO is more stochastic in nature with perhaps a 1–2-year predictability window (Weisheimer et al., 2022). Tide cycles like the 18.6-year nodal cycle, on the other hand, are deterministic with phasing that vary by region and tidal regime (see Haigh et al., 2011 for description). Where the nodal cycle is significant (Figure 2c), there is evidence of clustering of high tide flood frequencies near the peak in some locations (Figure 3). The nodal cycle peaked around 2013 ± 4 years, 2006 ± 2 years and 2007 ± 5 years along U.S. Atlantic/Gulf, U.S. West and Pacific Island coasts, respectively, and will again do so about every 19 years thereafter and affect EWL probabilities including sub-annual high tide flooding (P. R. Thompson et al., 2021). But, not all EWL variability has been diagnosed in this study. To do so requires more customized indices (e.g., Rashid & Wahl, 2020) like the Gulf Stream transport and its 5–10 cm effect on the location parameter (2–3 times higher than diagnosed in this study) along the Southeast U.S. (Sweet et al., 2016). Additional tidal harmonics could be examined, like the 4.4-year cycle related to the lunar perigee, which overrides the nodal cycle with a range about half the nodal cycle itself in some locations (Menéndez & Woodworth, 2010).

Though our models disentangle stochastic and deterministic from persistent trend influences on EWL probabilities, they do not quantify trends or variability in response to changes in storminess or intensity (i.e., changes in scale and shape parameters). Such changes like intensifying tropical storms (Seneviratne et al., 2021) could further affect rarer EWL probabilities in the future, which is of importance to federal agencies like the U.S. Army Corps of Engineers (Nadal-Caraballo et al., 2020). What our results do highlight are the time-dependent (location parameter) changes affecting the entire probability distribution of coastal EWLs. Meaning, the expected probabilities from high tides to rarer and higher-reaching EWLs all have and will continue to vary through time. In terms of intra-annual variability, our time-dependent models do quantify a pronounced seasonal cycle (19 ± 12 cm value change in location parameter—not shown) that varies by region and by process similar to the

findings of Menéndez and Woodworth (2010). In terms of monthly-to-annual predictions, high tide flood models that include the full range of tidal harmonics and/or predictable variability like ENSO are well positioned to help inform preparedness (Dusek et al., 2022; Sweet et al., 2018, 2021). In terms of the next 20–30 years, considering an equivalent SLR amount that bounds the envelope of interannual variability in EWL return level curves could further support assessment efforts for U.S. coastal communities (Collini et al., 2022; Hamlington et al., 2022; Sweet et al., 2022; P. R. Thompson et al., 2021).

Data Availability Statement

Tide gauge data in this study are provided by NOAA (2023b) and the University of Hawaii Sea Level Center (Caldwell et al., 2015). Climate indices used in this study are provided by NOAA (2023a). Models results for each location are available at the University of Hawaii (UH, 2024).

Acknowledgments

Support was provided from the US Department of Defense (DoD) Strategic Environmental Research and Development Program (SERDP) under Project RC-2644. Jayantha Obeysekera had support from the Institute of Environment, FIU.

References

- Barnard, P. L., Erikson, L. H., Foxgrover, A. C., Finzi Hart, J. A., Limber, P., O'Neill, A. C., et al. (2019). Dynamic flood modeling essential to assess the coastal impacts of climate change. *Scientific Reports*, 9(1), 13. Article #4309. <https://doi.org/10.1038/s41598-019-40742-z>
- Barnard, P. L., Short, A. D., Harley, M. D., Splinter, K. D., Vitousek, S., Turner, I. L., et al. (2015). Coastal vulnerability across the Pacific dominated by El Niño/Southern oscillation. *Nature Geoscience*, 8(10), 801–807. <https://doi.org/10.1038/ngeo2539>
- Barnston, A. G., Chelliah, M., & Goldenberg, S. B. (1997). Documentation of a highly ENSO-related SST region in the equatorial Pacific: Research note. *Atmosphere-Ocean*, 35(3), 367–383. <https://doi.org/10.1080/07055900.1997.9649597>
- Beran, M. A., & Nozdryn-Plotnicki, M. K. (1977). Estimation of low return period floods. *Bulletin of the International Association of Scientific Hydrology*, 2, 275–282. <https://doi.org/10.1080/02626667709491717>
- Buchanan, M. K., Oppenheimer, M., & Kopp, R. E. (2017). Amplification of flood frequencies with local sea level rise and emerging flood regimes. *Environmental Research Letters*, 12(6), 064009. <https://doi.org/10.1088/1748-9326/aa6cb3>
- Caldwell, P. C., Merrifield, M. A., & Thompson, P. R. (2015). Sea level measured by tide gauges from global oceans — The Joint Archive for Sea Level Holdings (NCEI Accession 0019568) [Dataset], Version 5.5. NOAA National Centers for Environmental Information. <https://doi.org/10.7289/V5V40S7W>
- Church, J. A., Clark, P. U., Cazenave, A., Gregory, J. M., Jevrejeva, S., Levermann, A., et al. (2013). Sea level change. In T. F. Stocker, D. Qin, G.-K. Plattner, M. Tignor, S. K. Allen, J. Boschung, et al. (Eds.), *Climate change 2013: The physical science basis. Contribution of Working Group I to the fifth assessment report of the Intergovernmental Panel on Climate Change*. Cambridge University Press. Retrieved from https://www.ipcc.ch/site/assets/uploads/2018/02/WG1AR5_Chapter13_FINAL.pdf
- Coles, S., Bawa, J., Trenner, L., & Dorazio, P. (2001). *An introduction to statistical modeling of extreme values* (Vol. 208, p. 208). Springer. <https://doi.org/10.1007/978-1-4471-3675-0>
- Collini, R. C., Carter, J., Auermuller, L., Engeman, L., Hintzen, K., Gambill, J., et al. (2022). Application guide for the 2022 sea level rise technical report. National Oceanic and Atmospheric Administration Office for Coastal Management, Mississippi–Alabama Sea Grant Consortium (MASGP-22-028), and Florida Sea Grant (SGEB 88). Retrieved from <https://oceanservice.noaa.gov/hazards/sealevelrise/noaa-nos-techrpt02-globalregional-SLR-scenarios-US-application-guide.pdf>
- Dangendorf, S., Hendricks, N., Sun, Q., Klinck, J., Ezer, T., Frederikse, T., et al. (2023). Acceleration of US Southeast and Gulf coast sea-level rise amplified by internal climate variability. *Nature Communications*, 14(1), 1–11. <https://doi.org/10.1038/s41467-023-37649-9>
- Dusek, G., Sweet, W. V., Widlansky, M. J., Thompson, P. R., & Marra, J. J. (2022). A novel statistical approach to predict seasonal high tide flooding. *Frontiers in Marine Science*, 9, 1073792. <https://doi.org/10.3389/fmars.2022.1073792>
- Enfield, D. B., Mestas, A. M., Mayer, D. A., & Cid-Serrano, L. (1999). How ubiquitous is the dipole relationship in tropical Atlantic sea surface temperatures? *Journal of Geophysical Research*, 104(C4), 7841–7848. <https://doi.org/10.1029/1998jc900109>
- FEMA. (2016). *Guidance for flood risk analysis mapping: Coastal flood frequency and extreme value analysis*. Guidance Document 76 (p. 22). Federal Emergency Management Agency. Retrieved from https://www.fema.gov/sites/default/files/2020-02/Coastal_Flood_Frequency_and_Extreme_Value_Analysis_Guidance_Nov_2016.pdf
- Fox-Kemper, B., Hewitt, H. T., Xiao, C., Aðalgeirsdóttir, G., Drijfhout, S. S., Edwards, T. L., et al. (2021). Ocean, cryosphere and sea level change. In V. MassonDelmotte, P. Zhai, A. Pirani, S. L. Connors, C. Péan, S. Berger, et al. (Eds.), *Climate change 2021: The physical science basis. Contribution of Working Group I to the sixth assessment report of the Intergovernmental Panel on Climate Change* (pp. 1211–1362). Cambridge University Press. <https://doi.org/10.1017/9781009157896.011>
- Ghanbari, M., Arabi, M., Obeysekera, J., & Sweet, W. (2019). A coherent statistical model for coastal flood frequency analysis under nonstationary sea level conditions. *Earth's Future*, 7(2), 162–177. <https://doi.org/10.1029/2018ef001089>
- Haigh, I. D., Eliot, M., & Pattiaratchi, C. (2011). Global influences of the 18.61 year nodal cycle and 8.85 year cycle of lunar perigee on high tidal levels. *Journal of Geophysical Research*, 116(C6), C06025. <https://doi.org/10.1029/2010jc006645>
- Hall, J. A., Gill, S., Obeysekera, J., Sweet, W., Knuutti, K., & Marburger, J. (2016). *Regional sea level scenarios for coastal risk management: Managing the uncertainty of future sea level change and extreme water levels for Department of Defense Coastal Sites Worldwide* (p. 224). U. S. Department of Defense, Strategic Environmental Research and Development Program. Retrieved from https://climateandsecurity.files.wordpress.com/2014/01/regional-sea-level-scenarios-for-coastal-risk-management_managing-uncertainty-of-future-sea-level-change-and-extreme-water-levels-for-department-of-defense.pdf
- Hamlington, B. D., Chambers, D. P., Frederikse, T., Dangendorf, S., Fournier, S., Buzzanga, B., & Nerem, R. S. (2022). Observation-based trajectory of future sea level for the coastal United States tracks near high-end model projections. *Communications Earth & Environment*, 3(1), 230. <https://doi.org/10.1038/s43247-022-00537-z>
- Hunter, J. (2012). A simple technique for estimating an allowance for uncertain sea-level rise. *Climatic Change*, 113(2), 239–252. <https://doi.org/10.1007/s10584-011-0332-1>
- Hurrell, J. W. (1995). Decadal trends in the North Atlantic Oscillation: Regional temperatures and precipitation. *Science*, 269(5224), 676–679. <https://doi.org/10.1126/science.269.5224.676>

- Izaguirre, C., Méndez, F. J., Menéndez, M., & Losada, I. J. (2011). Global extreme wave height variability based on satellite data. *Geophysical Research Letters*, 38(10), L10607. <https://doi.org/10.1029/2011gl047302>
- Karegar, M. A., Dixon, T. H., Malservisi, R., Kusche, J., & Engelhart, S. E. (2017). Nuisance flooding and relative sea-level rise: The importance of present-day land motion. *Scientific Reports*, 7(1), 1–9. <https://doi.org/10.1038/s41598-017-11544-y>
- Kirk, K., Dusek, G., Tissot, P., & Sweet, W. (2022). An approach to approximate wave height from acoustic tide gauges. *Journal of Atmospheric and Oceanic Technology*, 39(6), 721–738. <https://doi.org/10.1175/jtech-d-20-0212.1>
- Kopp, R. E., Horton, R. M., Little, C. M., Mitrovica, J. X., Oppenheimer, M., Rasmussen, D. J., et al. (2014). Probabilistic 21st and 22nd century sea-level projections at a global network of tide-gauge sites. *Earth's Future*, 2(8), 383–406. <https://doi.org/10.1002/2014EF000239>
- Li, S., Wahl, T., Barroso, A., Coats, S., Dangendorf, S., Piecuch, C., et al. (2022). Contributions of different sea-level processes to high-tide flooding along the U.S. coastline. *Journal of Geophysical Research: Oceans*, 127(7), e2021JC018276. <https://doi.org/10.1029/2021JC018276>
- Lobeto, H., Semedo, A., Lemos, G., Dastgheib, A., Menendez, M., Ranasinghe, R., & Bidlot, J. R. (2024). Global coastal wave storminess. *Scientific Reports*, 14(1), 3726. <https://doi.org/10.1038/s41598-024-51420-0>
- Mantua, N. J., Hare, S. R., Zhang, Y., Wallace, J. M., & Francis, R. C. (1997). A Pacific decadal climate oscillation with impacts on salmon. *Bulletin of the American Meteorological Society*, 78(6), 1069–1079. [https://doi.org/10.1175/1520-0477\(1997\)078<1069:apicow>2.0.co;2](https://doi.org/10.1175/1520-0477(1997)078<1069:apicow>2.0.co;2)
- Marra, J. J., Sweet, W. V., Leuliette, E., Kruk, M., Genz, A. S., Storlazzi, C. D., et al. (2023). Advancing best practices for the analysis of the vulnerability of military installations in the Pacific basin to coastal flooding under a changing climate – RC-2644. Final Report for the U.S. Department of Defense Strategic Environmental Research and Development Program. January 25, 2023 (p. 543).
- May, C. L., Osler, M. S., Stockdon, H. F., Barnard, P. L., Callahan, J. A., Collini, R. C., et al. (2023). Ch. 9. Coastal effects. In A. R. Crimmins, C. W. Avery, D. R. Easterling, K. E. Kunkel, B. C. Stewart, & T. K. Maycock (Eds.), *Fifth National Climate Assessment*. U.S. Global Change Research Program. <https://doi.org/10.7930/NCA5.2023.CH9>
- Méndez, F. J., Menéndez, M., Luceño, A., & Losada, I. J. (2006). Estimation of the long-term variability of extreme significant wave height using a time-dependent peak over threshold (POT) model. *Journal of Geophysical Research*, 111(C7), C07024. <https://doi.org/10.1029/2005jc003344>
- Méndez, F. J., Menéndez, M., Luceño, A., & Losada, I. J. (2007). Analyzing monthly extreme sea levels with a time-dependent GEV model. *Journal of Atmospheric and Oceanic Technology*, 24(5), 894–911. <https://doi.org/10.1175/jtech2009.1>
- Menendez, M., Mendez, F. J., Izaguirre, C., Luceño, A., & Losada, I. J. (2009). The influence of seasonality on estimating return values of significant wave height. *Coastal Engineering*, 56(3), 211–219. <https://doi.org/10.1016/j.coastaleng.2008.07.004>
- Menendez, M., Mendez, F. J., & Losada, I. J. (2009). Forecasting seasonal to interannual variability in extreme sea levels. *ICES Journal of Marine Science*, 66(7), 1490–1496. <https://doi.org/10.1093/icesjms/ffsp095>
- Menéndez, M., & Woodworth, P. L. (2010). Changes in extreme high water levels based on a quasi-global tide-gauge data set. *Journal of Geophysical Research*, 115(C10), C10011. <https://doi.org/10.1029/2009JC005997>
- Moftakhari, H. R., AghaKouchak, A., Sanders, B. F., Feldman, D. L., Sweet, W., Matthew, R. A., & Luke, A. (2015). Increased nuisance flooding along the coasts of the United States due to sea level rise: Past and future. *Geophysical Research Letters*, 42(22), 9846–9852. <https://doi.org/10.1002/2015gl066072>
- Moritz, H., White, K., Gouldby, B., Sweet, W., Ruggiero, P., Gravens, M., et al. (2015). USACE adaptation approach for future coastal climate conditions. *Proceedings of the Institution of Civil Engineers-Maritime Engineering*, 168(3), 111–117. <https://doi.org/10.1680/jmaen.15.00015>
- Muis, S., Verlaan, M., Winsemius, H. C., Aerts, J. C. J. H., & Ward, P. J. (2016). A global reanalysis of storm surges and extreme sea levels. *Nature Communications*, 7(1), 11969. <https://doi.org/10.1038/ncomms11969>
- Nadal-Caraballo, N. C., Campbell, M. O., Gonzalez, V. M., Torres, M. J., Melby, J. A., & Taflanidis, A. A. (2020). Coastal hazards system: A probabilistic coastal hazard analysis framework. *Journal of Coastal Research*, 95(SI), 1211–1216. <https://doi.org/10.2112/SI95-235.1>
- NOAA. (2023a). Climate indices: Monthly atmospheric and ocean time series [Dataset]. Retrieved from <https://psl.noaa.gov/data/climateindices/list/>
- NOAA. (2023b). Hourly tide gauge data [Dataset]. *National Oceanic and Atmospheric Administration*. Retrieved from <https://tidesandcurrents.noaa.gov/>
- Obeysekera, J., & Salas, J. (2020). Hydrologic designs for extreme events under nonstationarity. In J. R. Olsen & K. T. Adamec (Eds.), *Engineering methods for precipitation under a changing climate* (pp. 63–82). American Society of Civil Engineers. <https://doi.org/10.1061/9780784415528.ch04>
- Oppenheimer, M., Glavovic, B. C., Hinkel, J., van de Wal, R., Magnan, A. K., Abd-Elgawad, A., et al. (2019). Sea level rise and implications for low-lying islands, coasts and communities. In H.-O. Pörtner, D. C. Roberts, V. Masson-Delmotte, P. Zhai, M. Tignor, E. Poloczanska, et al. (Eds.), *IPCC special report on the ocean and cryosphere in a changing climate* (pp. 321–445). Cambridge University Press. <https://doi.org/10.1017/9781009157964.006>
- Rashid, M. M., & Wahl, T. (2020). Predictability of extreme sea level variations along the US coastline. *Journal of Geophysical Research: Oceans*, 125(9), e2020JC016295. <https://doi.org/10.1029/2020jc016295>
- Rashid, M. M., Wahl, T., Chambers, D. P., Calafat, F. M., & Sweet, W. V. (2019). An extreme sea level indicator for the contiguous United States coastline. *Scientific Data*, 6(1), 326. <https://doi.org/10.1038/s41597-019-0333-x>
- Riahi, K., Schaeffer, R., Arango, J., Calvin, K., Guivarch, C., Hasegawa, T., et al. (2022). Mitigation pathways compatible with long-term goals. In P. R. Shukla, J. Skea, R. Slade, A. Al Khourdajie, R. van Diemen, D. McCollum, et al. (Eds.), *IPCC, 2022: Climate change 2022: Mitigation of climate change. Contribution of Working Group III to the sixth assessment report of the Intergovernmental Panel on Climate Change*. Cambridge University Press. <https://doi.org/10.1017/9781009157926.005>
- Rice, J. (1994). *Mathematical statistics and data analysis* (2nd ed.). Duxbury Press.
- Salas, J. D., Obeysekera, J., & Vogel, R. M. (2018). Techniques for assessing water infrastructure for nonstationary extreme events: A review. *Hydrological Sciences Journal*, 63(3), 325–352. <https://doi.org/10.1080/02626667.2018.1426858>
- Seneviratne, S. I., Zhang, X., Adnan, M., Badi, W., Dereczynski, C., Di Luca, A., et al. (2021). Weather and climate extreme events in a changing climate. In V. Masson-Delmotte, P. Zhai, A. Pirani, S. L. Connors, C. Péan, S. Berger, et al. (Eds.), *Climate change 2021: The physical science basis. Contribution of Working Group I to the sixth assessment report of the Intergovernmental Panel on Climate Change* (pp. 1513–1766). Cambridge University Press. <https://doi.org/10.1017/9781009157896.013>
- Serafin, K. A., & Ruggiero, P. (2014). Simulating extreme total water levels using a time-dependent, extreme value approach. *Journal of Geophysical Research: Oceans*, 119(9), 6305–6329. <https://doi.org/10.1002/2014jc010093>
- Serafin, K. A., Ruggiero, P., & Stockdon, H. F. (2017). The relative contribution of waves, tides, and nontidal residuals to extreme total water levels on US West Coast sandy beaches. *Geophysical Research Letters*, 44(4), 1839–1847. <https://doi.org/10.1002/2016gl071020>
- Shope, J. B., Erikson, L. H., Barnard, P. L., Storlazzi, C. D., Serafin, K. A., Doran, K. J., et al. (2022). Characterizing storm-induced coastal change hazards along the United States West Coast. *Nature Scientific Data*, 9(1), 20. Paper #224. <https://doi.org/10.1038/s41597-022-01313-6>

- Smith, C. A., & Sardeshmukh, P. (2000). The effect of ENSO on the intraseasonal variance of surface temperature in winter. *International Journal of Climatology*, *20*(13), 1543–1557. [https://doi.org/10.1002/1097-0088\(20001115\)20:13<1543::aid-joc579>3.0.co;2-a](https://doi.org/10.1002/1097-0088(20001115)20:13<1543::aid-joc579>3.0.co;2-a)
- Storlazzi, C. D., Gingerich, S. B., Van Dongeren, A. P., Cheriton, O. M., Swarzenski, P. W., Quataert, E., et al. (2018). Most atolls will be uninhabitable by the mid-21st century because of sea-level rise exacerbating wave-driven flooding. *Science Advances*, *4*(4), eaap9741. <https://doi.org/10.1126/sciadv.aap9741>
- Sweet, W. V., Dusek, G., Obeysekera, J., & Marra, J. J. (2018). *Patterns and projections of high tide flooding along the U.S. coastline using a common impact threshold*. NOAA Technical Report NOS CO-OPS 086 (p. 44). National Oceanic and Atmospheric Administration, National Ocean Service. Retrieved from https://tidesandcurrents.noaa.gov/publications/techrpt86_PaP_of_HTFflooding.pdf
- Sweet, W. V., Hamlington, B. D., Kopp, R. E., Weaver, C. P., Barnard, P. L., Bekaert, D., et al. (2022). *Global and regional sea level rise scenarios for the United States: Updated mean projections and extreme water level probabilities along U.S. coastlines*. NOAA Technical Report NOS 01 (p. 111). National Oceanic and Atmospheric Administration, National Ocean Service. Retrieved from <https://oceanservice.noaa.gov/hazards/sealevelrise/noaa-nos-techrpt01-global-regional-SLR-scenarios-US.pdf>
- Sweet, W. V., Menendez, M., Genz, A., Obeysekera, J., Park, J., & Marra, J. J. (2016). In tide's way: Southeast Florida's September 2015 sunny-day flood. *Bulletin of the American Meteorological Society*, *97*(12), S25–S30. <https://doi.org/10.1175/bams-d-16-0117.1>
- Sweet, W. V., & Park, J. (2014). From the extreme to the mean: Acceleration and tipping points of coastal inundation from sea level rise. *Earth's Future*, *2*(12), 579–600. <https://doi.org/10.1002/2014EF000272>
- Sweet, W. V., Park, J., Gill, S., & Marra, J. (2015). New ways to measure waves and their effects at NOAA tide gauges: A Hawaiian-network perspective. *Geophysical Research Letters*, *42*(21), 9355–9361. <https://doi.org/10.1002/2015gl066030>
- Sweet, W. V., Simon, S., Dusek, G., Marcy, D., Brooks, W., Pendleton, M., & Marra, J. (2021). *2021 State of high tide flooding and annual outlook*. NOAA High Tide Flooding Report (p. 28). National Oceanic and Atmospheric Administration, National Ocean Service. Retrieved from https://tidesandcurrents.noaa.gov/publications/2021_State_of_High_Tide_Flooding_and_Annual_Outlook_Final.pdf
- Sweet, W. V., & Zervas, C. (2011). Cool-season sea level anomalies and storm surges along the US East Coast: Climatology and comparison with the 2009/10 El Niño. *Monthly Weather Review*, *139*(7), 2290–2299. <https://doi.org/10.1175/mwr-d-10-05043.1>
- Taherkhani, M., Vitousek, S., Barnard, P. L., Frazer, N., Anderson, T. R., & Fletcher, C. H. (2020). Sea-level rise exponentially increases coastal flood frequency. *Scientific Reports*, *10*(1), 6466. <https://doi.org/10.1038/s41598-020-62188-4>
- Tebaldi, C., Strauss, B. H., & Zervas, C. E. (2012). Modelling sea level rise impacts on storm surges along US coasts. *Environmental Research Letters*, *7*(1), 014032. <https://doi.org/10.1088/1748-9326/7/1/014032>
- Thompson, D. W. J., & Wallace, J. M. (1998). The Arctic Oscillation signature in the wintertime geopotential height and temperature fields. *Geophysical Research Letters*, *25*(9), 1297–1300. <https://doi.org/10.1029/98gl00950>
- Thompson, P. R., Mitchum, G. T., Vonesch, C., & Li, J. (2013). Variability of winter storminess in the eastern United States during the twentieth century from tide gauges. *Journal of Climate*, *26*(23), 9713–9726. <https://doi.org/10.1175/jcli-d-12-00561.1>
- Thompson, P. R., Widlansky, M. J., Hamlington, B. D., Merrifield, M. A., Marra, J. J., Mitchum, G. T., & Sweet, W. (2021). Rapid increases and extreme months in projections of United States high-tide flooding. *Nature Climate Change*, *11*, 1–7. <https://doi.org/10.1038/s41558-021-01077-8>
- Thompson, P. R., Widlansky, M. J., Leuliette, E., Chambers, D. P., Sweet, W., Hamlington, B. D., et al. (2023). Sea-level variability and change [in “State of the climate in 2022”]. *Bulletin of the American Meteorological Society*, *104*(9), S173–S176. <https://doi.org/10.1175/BAMS-D-23-0076.2>
- UH. (2024). Annual amplitudes and 2019/2020 return levels [Dataset]. Retrieved from <https://apdrc.soest.hawaii.edu/SERDP/Implications/>
- Vitousek, S., Barnard, P. L., Fletcher, C. H., Frazer, N., Erikson, L., & Storlazzi, C. D. (2017). Doubling of coastal flooding frequency within decades due to sea-level rise. *Scientific Reports*, *7*(1), 1–9. <https://doi.org/10.1038/s41598-017-01362-7>
- Vousdoukas, M. I., Mentaschi, L., Voukouvalas, E., Verlaan, M., Jevrejeva, S., Jackson, L. P., & Feyen, L. (2018). Global probabilistic projections of extreme sea levels show intensification of coastal flood hazard. *Nature Communications*, *9*(1), 2360. <https://doi.org/10.1038/s41467-018-04692-w>
- Wahl, T., & Chambers, D. P. (2016). Climate controls multidecadal variability in US extreme sea level records. *Journal of Geophysical Research: Oceans*, *121*(2), 1274–1290. <https://doi.org/10.1002/2015jc011057>
- Wahl, T., Haigh, I. D., Nicholls, R. J., Arns, A., Dangendorf, S., Hinkel, J., & Slangen, A. B. (2017). Understanding extreme sea levels for broad-scale coastal impact and adaptation analysis. *Nature Communications*, *8*(1), 16075. <https://doi.org/10.1038/ncomms16075>
- Wallace, J. M., & Gutzler, D. S. (1981). Teleconnections in the geopotential height field during the Northern Hemisphere winter. *Monthly Weather Review*, *109*(4), 784–812. [https://doi.org/10.1175/1520-0493\(1981\)109<0784:titghf>2.0.co;2](https://doi.org/10.1175/1520-0493(1981)109<0784:titghf>2.0.co;2)
- Weisheimer, A., Balmaseda, M. A., Stockdale, T. N., Mayer, M., Sharmila, S., Hendon, H., & Alves, O. (2022). Variability of ENSO forecast skill in 2-year global reforecasts over the 20th century. *Geophysical Research Letters*, *49*(10), e2022GL097885. <https://doi.org/10.1029/2022gl097885>
- Zervas, C. (2013). Extreme water levels of the United States 1893–2010. NOAA Technical Report NOS CO-OPS 67 (p. 56). Appendices I–VIII.